Modeling LiH potential-energy curves: An approach based on integration in finite space

S. N. Altunata and R. W. Field*
Department of Chemistry, Massachusetts Institute of Technology, Cambridge, Massachusetts 02139
(Received 29 August 2002; published 28 February 2003)

In this paper, we introduce a finite-space integration method to shed physical insight into the interactions of a Rydberg electron with a molecular ion core, as sampled by the potential-energy curves (PECs) of various electronic states of LiH. We postulate that these interactions are dominated by two independent electron-atom processes: (1) scattering of the Rydberg electron at negative energy solely off of the lithium atomic core and (2) a transition from the lithium scattering state to the lithium valence orbital necessarily accompanied by an excitation of the hydrogen atom. It is shown that the ratio of the amplitudes for the occurrences of these two processes can be obtained by means of bounded integrations inside a small region of space where the electron-electron repulsion term in the Hamiltonian is dominant. Our theory and approximations are verified by a comparison of derived potential-energy curves with those produced by *ab initio* calculations as well as another empirical model that uses the Fermi approximation. It is observed that the complicated features of the PECs, which reflect the nodal structure of the Rydberg orbitals, are reproduced well within our treatment.

DOI: 10.1103/PhysRevA.67.022507 PACS number(s): 31.15.−p, 31.10.+z

I. INTRODUCTION

Excited electronic states of diatomic molecules continue to be a challenging subject of study. Although very accurate electronic structure computations can be made by *ab initio* methods, purely numerical approaches rarely provide a transparent ''zero-order'' description of the mechanisms of the many-body interactions. The main reason for this difficulty is that an analysis that is performed state by state cannot capture a global picture of structure and dynamics. The identification and classification of the most important physical processes remain a difficult task because the simplest dynamical processes are often encoded in a complicated way in the totality of the potential-energy curves of excited electronic states. Thus, rather than treating the problem rigorously and accurately in a state by state way, a more approximate, global approach is needed to reveal the most important physical processes.

In this work, we develop such an analysis for the triplet-Rydberg states of the LiH molecule. Our central goal is to explain the global electronic structure of LiH, from its low-lying to higher-Rydberg states, in a unified way. This molecule has been extensively studied, both experimentally and computationally, and its properties are very well understood. In a recent study, Dickinson and Gadèa [1] have shown that the electronic structure of LiH can be explained within the Fermi approximation. That approximation rests on the premise that electronic motion is dominated by a simple dynamical process, namely, the collision of a Rydberg electron localized on the lithium atom with the hydrogen atom.[1] The Fermi approximation is capable of predicting the electronic structure for low-lying Rydberg states, however, it cannot be used to describe the evolution of the electronic structure to higher-Rydberg states. The reason for this is that the Fermi approximation makes use of the perturbation expansion and the mixing angles remain finite for an infinity of states in the high principal quantum number limit.

In order to avoid this difficulty and to treat low- and high-Rydberg states in a unified way, we incorporate the channel wave-function formalism of quantum-defect theory directly into the electronic structure calculation [2]. The usefulness of the potential-energy curves (PECs) of the higher states for the determination of the quantum-defect curves and their energy dependence is explained in Ref. [3].

We postulate the existence of *two* atom-based processes as the dominant interactions in the LiH molecule. These two processes are expressed globally as channel wave functions [4] in our formalism. We then show that the coupling between the two channels is evaluated by means of bounded integrations inside a small region of space where the electron-electron repulsion term is large. Consequently, we derive a bounded space integration formula to be used in the approximate calculation of the global electronic structure. Hence, this bounded space integration formula shows that the solution of the Schrödinger equation in this special, compact region of space contains the most important information about dynamical processes in the molecule and leads to new physical insight that was not immediately available in the previous treatments. In Sec. IV, we compare the potential-energy curves obtained by our bounded space integration method to previous *ab initio* calculations as well as to the Fermi approximation results and discuss the overall qualitative agreement between the PECs determined by the various approaches.

II. THEORY

We begin by considering a Rydberg state of a LiH molecule at infinite nuclear separation. From the atomic point of view such a state will be reached by the excitation of a Li$(2s)$ electron. Now we imagine the two atoms approach-

*Author to whom correspondence should be addressed.

[1]In the Fermi approximation, the hydrogen atom is viewed as a passive, nonpolarizable δ function. In Sec. II, we treat the H atom dynamically by allowing its structure to change during the electron-scattering process.

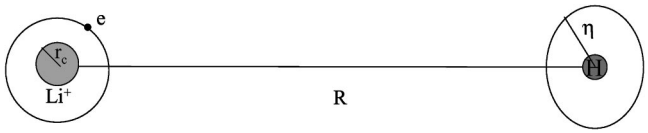

FIG. 1. Lithium and hydrogen atoms at large internuclear separation.

ing each other with zero total angular momentum about the center of mass (see Fig. 1).

At large internuclear separation, the lithium Rydberg electron does not ''feel'' the presence of the hydrogen atom. The Rydberg electron is in orbit about Li^+ and its wave function is given by a superposition of Coulomb partial waves [5] that acquire phase shifts as the electron scatters off the lithium atomic-ion core. As the H atom approaches the Li atom, it increasingly perturbs the motion of the Rydberg electron. One way to model this is to view the hydrogen atom as a passive perturber, which is accomplished by the addition of a pseudopotential [1] to the lithium atomic Hamiltonian, and the use of perturbation theory to obtain the potential-energy curve of interaction between the two nuclei. Instead, we model the effect of the approaching H atom by a channel wave function of the Rydberg electron [4], which expresses the exchange of energy between the Rydberg electron and the ground-state hydrogen atom by allowing for the possibility of excitation of the hydrogen atom. In doing so, we identify, at intermediate internuclear separation, an ion-core structure interacting with a Rydberg electron through two channels.

(1) The electron exits the molecular ion core with an asymptotic phase shift that it acquires inside the Li^+ atomic core, leaving behind a Li^+H ion-core structure.

(2) The electron settles into the $Li(2s)$ valence shell, causing an excitation of the H atom. This excitation is manifested as a transition of the ion-core electronic state from its ground-state Li^+H configuration to an excited state in which the electronic charge density shifts toward a LiH^+ configuration.

We ignore all other energetically open channels, such as those leading to a rotation or vibration of the ion core about the center of mass and assume that the two distinct electron-atom scattering processes are associated with the same rovibrational state of the nuclei.

III. FORMALISM

Consider the LiH molecule (Fig. 2). The total Hamiltonian for the system is

$$\mathcal{H}=\mathcal{H}_1+\mathcal{H}_2+\frac{1}{r_{12}}+\frac{p_{\mathrm{Li}}^2}{2m_{\mathrm{Li}}}+\frac{p_{\mathrm{H}}^2}{2m_{\mathrm{H}}}+\frac{1}{R}, \tag{1}$$

where subscripts 1 and 2 refer to the valence electrons.[2] We treat the inner electrons as an electrostatic charge density

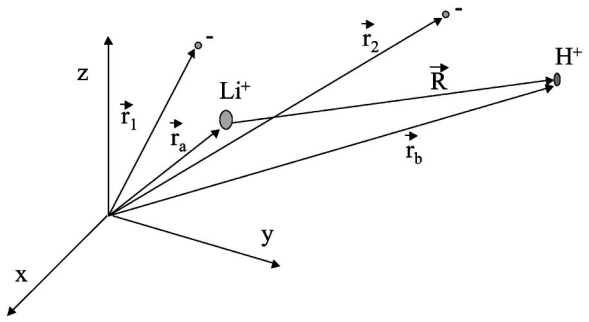

FIG. 2. LiH molecule. The coordinates of the particles are labeled by vectors with respect to laboratory fixed coordinate axes.

about the Li nucleus and model this charge density with an effective potential. Thus we let

$$\mathcal{H}_n=-\frac{1}{r_{an}}-\frac{2e^{-2.13r_{an}}}{r_{an}}-\frac{1}{r_{bn}}+\frac{p_n^2}{2m_e}. \tag{2}$$

Here r_{an} and r_{bn} are the distances of the nth electron from the lithium and hydrogen nuclei, respectively. The effective potential term $-(1/r_{an})-(2e^{-2.13r_{an}}/r_{an})$ describes the interaction of an electron with Li^+ [6]. Based on the two-channel hypothesis of Sec. II, we make the following ansatz for an electronic wave function:

$$\psi^{el}(\tau)=\psi_+^{(1)}(\vec{r}_2-\vec{r}_b)\psi_{n*}(\vec{r}_1-\vec{r}_a;|\vec{r}_1-\vec{r}_a|>r_c) + \psi_+^{(2)}(\vec{r}_2;\vec{R})\psi_{2s}(\vec{r}_1-\vec{r}_b;\vec{R};|\vec{r}_1-\vec{r}_b|>\eta), \tag{3}$$

where $\vec{R}=\vec{r}_b-\vec{r}_a$, $\psi_+^{(1)}$ and $\psi_+^{(2)}$ are the two ion-core eigenstates which solve the Schrödinger equation for the Hamiltonian in terms of one-electron operators:

$$\mathcal{H}_2\psi_+^1(\vec{r}_2-\vec{r}_b)=E_1^+(R)\psi_+^1(\vec{r}_2-\vec{r}_b),$$

$$\mathcal{H}_2\psi_+^2(\vec{r}_2;\vec{R})=E_2^+(R)\psi_+^2(\vec{r}_2;\vec{R}), \tag{4}$$

where $E_i^+(R)+1/R$, for $i=1$ and 2, are the potential-energy curves for the molecular ion in the two different ion-core eigenstates. The ion-core eigenstates are orthonormal,

$$\langle\psi_+^{(i)}|\psi_+^{(j)}\rangle=\delta_{ij}, \tag{5}$$

and they are adiabatic,

$$\boldsymbol{\nabla}_R\psi_+^{(i)}=\nabla_R^2\psi_+^{(i)}=0. \tag{6}$$

Equation (3) clearly expresses the two dominant physical processes. The first term in this expression, $\psi_+^1(\vec{r}_2-\vec{r}_b)\psi_{n*}(\vec{r}_1-\vec{r}_a)$ describes an electron in a Rydberg state interacting with a Li^+ atomic core, and should be dominant in the wave function at large internuclear separation. As the two atoms approach each other, another process becomes significant, namely, the excitation of the hydrogen atom. This

[2]See Fig. 2 for labels for the coordinates of all particles.

process is expressed by the second term in the wave function, which is implicitly R dependent. As will be demonstrated, the main reason for this R dependence is the nonlocal nature of the excitation process, namely, the electron correlation term, $1/r_{12}$, in the Hamiltonian.

Notice also that this wave function is defined in an outer region of space that excludes certain volumes about each of the nuclei (see Fig. 1). The reason for imposing such a restriction is to be able to evaluate the matrix elements of $1/r_{12}$, which simplify in the outer region. This simplification occurs because the two ion-core states express the two possible localizations of the inner charge density about the individual nuclei. The scattering from Li^+ is associated with the ion-core eigenstate $\psi_+^{(1)}$, and this wave function describes an electrostatic charge density localized about the H atom that corresponds to a Li^+H ion core. Similarly, $\psi_+^{(2)}$ is associated with the process of hydrogen excitation, and this wave function implies the presence of a charge density on the Li atom and an ion core with a strong LiH^+ character. This rearrangement of the inner charge density is due to an *exchange* of energy between the Rydberg electron and the stationary inner electron. The term in the Hamiltonian that is responsible for such an exchange of energy is the electron-electron repulsion term, $1/r_{12}$. In the outer region, the matrix elements of $1/r_{12}$ can be evaluated using the assumed extreme localization properties of the ion-core states:

$$\left\langle \psi_+^{(1)} \middle| \frac{1}{r_{12}} \middle| \psi_+^{(1)} \right\rangle = \frac{1}{r_{b1}} - \frac{\alpha}{2r_{b1}^4},$$

$$\left\langle \psi_+^{(2)};\vec{R} \middle| \frac{1}{r_{12}} \middle| \psi_+^{(2)};\vec{R} \right\rangle = \frac{1}{r_{a1}} + 2\frac{e^{-2.13r_{a1}}}{r_{a1}} - \frac{\beta}{2r_{a1}^4},$$

$$\left\langle \psi_+^{(1)} \middle| \frac{1}{r_{12}} \middle| \psi_+^{(2)};\vec{R} \right\rangle = 0, \tag{7}$$

where $\alpha = 4.50$ a.u. and $\beta = 164$ a.u. are, respectively, the ground-state polarizabilities of the H and Li atoms [7]. In evaluating the first two of these matrix elements, we assume that the Rydberg electron remains in a nonpenetrating orbit about a neutral spherical charge distribution. We then obtain analytical expressions for Eq. (7) matrix elements by noting that in the electric field of a negative point charge, the charge distribution of the neutral atom polarizes. The overall interaction energy between the outer electron and the electronic charge density about the neutral atom is given by the sum of a shielding term and a polarization term (proportional to $1/r^4$). The third matrix element is taken to be zero because $\psi_+^{(1)}$ and $\psi_+^{(2)}$ are localized on different nuclei and their overlap is essentially zero for sufficiently large internuclear separation. This approximation for the third integral will fail when R approaches zero. Therefore, we will assert that R is larger than a threshold value (~ 4 bohr). Accordingly in the outer region, exchange can be neglected because the two electrons are not permitted to sample the same region of space and they are localized on the different nuclei separated by $R > 4$ bohr. Given the matrix elements in Eq. (7), we can derive explicit equations for $\psi_n(\vec{r}_1 - \vec{r}_b;\vec{R})$ and $\psi_{n*}(\vec{r}_1 - \vec{r}_a)$ by assuming that a factorization of the form

$$\psi^{tot} = \psi^{el}\chi_n(\vec{R}), \tag{8}$$

solves the Schrödinger equation in the outer region for the molecular Hamiltonian in Eq. (1):

$$\begin{aligned}\mathcal{H}\psi^{tot} = E\psi^{tot} \Rightarrow & \left(\frac{P_R^2}{2\mu} + \mathcal{H}_1 + \mathcal{H}_2 + \frac{1}{r_{12}} + \frac{1}{R}\right)[\psi_+^1(\vec{r}_2 - \vec{r}_b) \\ & \times \psi_{n*}(\vec{r}_1 - \vec{r}_a) + \psi_+^{(2)}(\vec{r}_2;\vec{R})\psi_n(\vec{r}_1 - \vec{r}_b;\vec{R})]\chi_n(\vec{R}) \\ & = E[\psi_+^1(\vec{r}_2 - \vec{r}_b)\psi_{n*}(\vec{r}_1 - \vec{r}_a) \\ & + \psi_+^{(2)}(\vec{r}_2;\vec{R})\psi_n(\vec{r}_1 - \vec{r}_b;\vec{R})]\chi_n(\vec{R}).\end{aligned} \tag{9}$$

Taking the inner product of the terms in Eq. (9) with $\langle \psi_+^{(1)}|$ and using Eqs. (4)–(7), we obtain

$$\begin{aligned}&\left(\frac{P_R^2}{2\mu} + \frac{1}{R} + E_1^+(R) + \frac{p_1^2}{2m_e} - \frac{2e^{-2.13r_{a1}}}{r_{a1}} - \frac{1}{r_{a1}} - \frac{\alpha}{2r_{b1}^4}\right) \\ &\quad \times \psi_{n*}(\vec{r}_1 - \vec{r}_a)\chi_n(\vec{R}) = E\psi_{n*}(\vec{r}_1 - \vec{r}_a)\chi_n(\vec{R}).\end{aligned} \tag{10}$$

The presence of the $\alpha/2r_{b1}^4$ term in Eq. (10) causes the electronic and nuclear coordinates to be coupled in the differential equation. However, since α, the polarization of the H atom in its ground state, is *small* on the atomic scale, we expect (and require) the electronic wave function to exhibit only weak R dependence. If we neglect this R dependence altogether, then the Li^+-electron interaction becomes a purely atom-based scattering process and an approximate solution for $\psi_{n*}(\vec{r}_1 - \vec{r}_a)$ can be obtained. For $r_{a1} > r_c \approx 0.2$ bohr [see Fig. 1], the effective Li^+-electron interaction in Eq. (2) reduces approximately to $1/r_{a1}$. Since this interaction is spherically symmetric about the Li nucleus, the angular and the radial variables, as measured with respect to a coordinate system that takes the Li nucleus as its origin, can be separated in the differential equation. The reduced radial wave function of the Rydberg electron, denoted by $F(r_{a1})$, becomes a solution of the Coulomb radial equation,

$$\left(\frac{d^2}{dr_{a1}^2} - \frac{l(l+1)}{r_{a1}^2} + \frac{2}{r_{a1}} + 2\epsilon_1\right)F(r_{a1}) = 0. \tag{11}$$

The solution is then a superposition of two linearly independent Coulomb functions:

$$F(r_{a1}) = f_l(r_{a1},\epsilon_1)\cos[\pi\mu_l(\epsilon_1)] - g_l(r_{a1},\epsilon_1)\sin[\pi\mu_l(\epsilon_1)], \tag{12}$$

where $f_l(r_{a1})$ is the regular Coulomb function, which behaves like r_{a1}^{l+1} as r_{a1} approaches zero, and $g_l(r_{a1})$ is the

irregular Coulomb function which diverges as r_{a1}^{-l} as $r_{a1} \rightarrow 0$ [8]. The coefficients are chosen so that, for bound states at infinity, $F(r)$ diverges as

$$F(r) \underset{r\rightarrow\infty}{\longrightarrow} \xi(r) E^{\sqrt{-2\epsilon_1}r} \sin\left[\pi\left(\frac{1}{\sqrt{-2\epsilon_1}} + l + \mu_l(\epsilon_1)\right)\right], \tag{13}$$

which identifies $\pi\mu_l(\epsilon_1)$ as an asymptotic phase shift.[3] Demanding regularity as $r\rightarrow\infty$,

$$\epsilon_1 = \frac{-1}{2(n^*)^2},$$

$$n^* = n - \mu_{l,n}, \tag{14}$$

where n is an integer. For s waves on Li^+, the quantum defect turns out to be independent of n with the numerical value of 0.4 [6]. The explicit form of $\psi_{n*}(\vec{r}_1 - \vec{r}_a)$ becomes

$$\psi_{n*}(\vec{r}_1 - \vec{r}_a, |\vec{r}_1 - \vec{r}_a| > r_c) = \frac{1}{|\vec{r}_1 - \vec{r}_a|}[f_{\epsilon_1,l}(|\vec{r}_1 - \vec{r}_a|) \times \cos(\pi\mu_{l,n}) - g_{\epsilon_1,l}(|\vec{r}_1 - \vec{r}_a|) \times \sin(\pi\mu_{l,n})] Y_l^m(\theta_a, \phi_a), \tag{15}$$

where θ_a and ϕ_a are axial and azimuthal spherical polar coordinates with respect to the lab fixed coordinate axes, shown in Fig. 2, with the origin translated to the center of the lithium atom. Y_l^m is a spherical harmonic. This electronic wave function has no R dependence. It is an approximation to the exact solution in the sense that the interactions which would cause it to become R dependent, namely, the polarization of the H atom, were neglected. Accordingly, ϵ_1 is not an electronic binding energy for the molecule because its numerical value reflects only the properties of a Li^+ core. Nevertheless, we can define a rigorous electronic binding energy, in analogy to Eq. (14):

$$\epsilon_1(R) = \frac{-1}{2[n - \mu_{\mathrm{Li}}(R)]^2}, \tag{16}$$

where $\mu_{\mathrm{Li}}(R)$ is an R dependent quantum defect[4] which is determined here. This R dependence demonstrates that Li^+-electron scattering is not strictly an atom-based process but is affected by the presence of the H atom. An interaction which occurs exclusively through an atomic channel at infinite nuclear separation couples to a molecular channel at finite separation, and the strength of this coupling, in our formalism, is modeled by the R dependence of $\mu_{\mathrm{Li}}(R)$. From this point on, we take the electronic binding energy to be given by Eq. (16), although we continue to use the approximate R-independent representation for the wave function itself.

Similarly, we can take the inner product of the terms in Eq. (9) with $\langle \psi_+^{(2)}|$ and repeat the same procedure as above to obtain

$$\left(\frac{P_R^2}{2\mu} + \frac{1}{R} - \frac{1}{r_{b1}} + \frac{p_1^2}{2m_e} + E_2^{(+)}(R) - \frac{\beta}{2r_{a1}^4}\right) \times \psi_{2s}(\vec{r}_1 - \vec{r}_b; \vec{R})\chi_n(\vec{R}) = E\psi_{2s}(\vec{r}_1 - \vec{r}_b; \vec{R})\chi_n(\vec{R}). \tag{17}$$

Here β is the polarizability of the Li atom in its ground state and cannot be neglected since it is about 40 times larger than the value for hydrogen. The existence of this R dependence in the electronic coordinates of this equation forces the electronic wave function to be also R dependent. It is useful to employ a reduced expression for $\psi_n(\vec{r}_1 - \vec{r}_b; \vec{R})$ in the form of a product of two primitive functions:

$$\psi_{2s}(\vec{r}_1 - \vec{r}_b; \vec{R}) = A(R)\tilde{\psi}_{2s}(\vec{r}_1 - \vec{r}_b; \vec{R}), \tag{18}$$

where $A(R)$ is an oscillating term that may vary rapidly with R and $\tilde{\psi}_n(\vec{r}_1 - \vec{r}_b; \vec{R})$ is an envelope function which solves the clamped nuclei equation:

$$\left(\frac{p_1^2}{2m_e} - \frac{1}{r_{b1}} - \frac{\beta}{r_{a1}^4}\right)\tilde{\psi}_{2s}(\vec{r}_1 - \vec{r}_b; \vec{R}) = \epsilon_2(R)\tilde{\psi}_{2s}(\vec{r}_1 - \vec{r}_b; \vec{R}). \tag{19}$$

The term $A(R)$ describes the amplitude of occurrence of hydrogen excitation relative to the amplitude of pure scattering off of lithium as the two nuclei approach each other and can therefore be viewed as a mixing coefficient. A further condition on $A(R)$ is obtained by recalling that we expect, on physical grounds, the Li^+-electron scattering wavefunction term to dominate at infinite nuclear separation in Eq. (3). Thus we demand

$$\lim_{R\rightarrow\infty} A(R) = 0. \tag{20}$$

In analogy with Eq. (16), we express an electronic binding energy in the form

$$\epsilon_2(R) = -\frac{1}{2[1 - \mu_{\mathrm{H}}(R)]^2}, \tag{21}$$

where we have introduced an additional R dependent quantum-defect function $\mu_{\mathrm{H}}(R)$, which should also be

[3]We supress the subscript $(a1)$ on r in Eq. (13), since, in the asymptotic limit, the choice of origin is irrelevant.

[4]Note that the R-dependent quantum defect no longer has the meaning of an asymptotic phase shift but should be regarded as a fit parameter. Its general physical significance is explained in Ref. [12].

viewed as a fit parameter that models the hydrogenic excitation at a given internuclear separation. Equations (10) and (17) together imply the additional condition

$$U(R)=E_1^+(R)-\frac{1}{2[n-\mu_{\mathrm{Li}}(R)]^2}+\frac{1}{R}$$
$$=E_2^+(R)-\frac{1}{2[1-\mu_{\mathrm{H}}(R)]^2}+\frac{1}{R}, \qquad (22)$$

where $U(R)$ is the potential-energy curve for the motion of the nuclei, $E_1^+(R)$ and $E_2^+(R)$ are the two ion-core potential-energy curves in the two electronic eigenstates that correspond to Li^+H and LiH^+ structures, respectively. The eigenvalue equation for the nuclear motion becomes

$$\left(\frac{P_R^2}{2\mu}+\frac{1}{R}+U(R)\right)\chi_n(\vec{R})=E\chi_n(\vec{R}). \qquad (23)$$

An expression for $U(R)$ can readily be obtained if $A(R)$ is known. We now present a physical argument to calculate $A(R)$ which is subsequently used to calculate $U(R)$. We then refer to Eq. (22) to obtain the R-dependent quantum defects to model these two electronic channels that we have built into our theory.

In our formalism, the electron on the hydrogen atom can be collisionally excited from the ground state. This excitation can occur if the distance between the two electrons, r_{12}, is within an effective interaction length, η, for electron-hydrogen scattering, which is shown to be on the order of 3 bohr for the states under question. With respect to the exchange-neglected representation in Eq. (3), this corresponds to stating that the itinerant electron is found inside the sphere of radius η about the hydrogen atom during the excitation. Thus we restrict our attention to the region of space defined by

$$0<|\vec{r}_1-\vec{r}_b|<\eta. \qquad (24)$$

We refer to this region of space as the reaction zone. For electron positions inside the reaction zone, contributions to the exchange interaction are significant. Furthermore, the polarization approximation on the hydrogen atom fails. Assuming that the off-diagonal matrix elements of the Hamiltonian which get multiplied by $A(R)$ are small, we can write an approximate solution for the Scrödinger equation inside the reaction zone in the form

$$\phi_n^{el}(\tau)=(1-P_{12})[\psi_+^{(1)}(\vec{r}_2-\vec{r}_b)\psi_{n*}$$
$$\times(\vec{r}_1-\vec{r}_a;|\vec{r}_1-\vec{r}_b|<\eta)+A(R)\psi_+^{(2)}(\vec{r}_2-\vec{r}_a;\vec{R})$$
$$\times\tilde{\psi}_{2s}(\vec{r}_1-\vec{r}_b,0<|\vec{r}_1-\vec{r}_b|<\eta;\vec{R})]$$
$$+\sum_i B_i(R)\zeta_i(r_{12},\vec{r}_1-\vec{r}_b,\vec{r}_2-\vec{r}_b), \qquad (25)$$

where P_{12} is the electron permutation operator and the terms $\zeta_i(r_{12},\vec{r}_1-\vec{r}_b,\vec{r}_2-\vec{r}_b)$ describe the collision of the itinerant electron with the hydrogen atom in its ground state at zero energy and triplet symmetry [9]:

$$\lim_{r_{1b}\to\infty}\zeta_i(r_{12},\vec{r}_1-\vec{r}_b,\vec{r}_2-\vec{r}_b)$$
$$\sim\lim_{k\to 0}e^{-kr_{2b}}\frac{\sin\left[k\left(r_{1b}+\frac{\delta_o(k)}{k}\right)\right]}{r_{1b}}, \qquad (26)$$

where $\delta_o(k)$ is the s-wave partial phase shift. For simplicity, we neglect the scattering terms in the reaction zone electronic wave function. It is shown below by direct comparison to *ab initio* calculations that the error introduced from this simplification is not significant. In the absence of the scattering terms, one regains Eq. (17) after taking the inner product of $\mathcal{H}|\psi^{tot}\rangle$ with $\langle\psi_+^{(2)}|$ and ignoring the contribution from the Li^+ core. However, since the electronic coordinates of the itinerant electron are restricted to the region defined by Eq. (24), the lithium polarization term, $\beta/2r_{1a}^4$, that appears in Eq. (17) can be neglected. This is because the polarization term varies as the inverse fourth power of R and we require that $R>\eta\approx 3.5$ bohr. Therefore, the wave function for the itinerant electron reduces to

$$\tilde{\psi}_{2s}(\vec{r}_1-\vec{r}_b,0<|\vec{r}_1-\vec{r}_b|<\eta;\vec{R})=\psi_{2s}(\vec{r}_1-\vec{r}_b), \qquad (27)$$

where the R-independent $\psi_{2s}(\vec{r}_1-\vec{r}_b)$ is given by

$$\psi_{2s}(\vec{r}_1-\vec{r}_b)=\frac{1}{|\vec{r}_1-\vec{r}_b|}f_{2s}(|\vec{r}_1-\vec{r}_b|)Y_l^m(\theta_b,\phi_b), \qquad (28)$$

and θ_b and ϕ_b are axial and azimuthal spherical polar coordinates with respect to the lab fixed coordinate axes, shown in Fig. 2, with the origin translated to the center of the hydrogen atom. The electronic wave function in the reaction zone becomes

$$\phi_n^{el}(\tau)=\psi_+^{(1)}(\vec{r}_2-\vec{r}_b)\psi_{n*}(\vec{r}_1-\vec{r}_a)$$
$$+A(R)\psi_+^{(2)}(\vec{r}_2;\vec{R})\psi_{2s}(\vec{r}_1-\vec{r}_b). \qquad (29)$$

In Eq. (29), we have suppressed all of the complicated nonlocal effects and the only information that tells us that we are looking at a molecule in this wave function is the fact that the electrons are localized on the two different nuclei of the diatom. Now, let $\psi^{n'}(\vec{r}_1,\vec{r}_2,\vec{R})$ be an adiabatic eigenstate of the Born-Oppenheimer Hamiltonian defined by

$$\tilde{\mathcal{H}}=\mathcal{H}-\frac{\hat{P}_R^2}{2\mu}. \qquad (30)$$

Since the set of adiabatic eigenstates at any internuclear separation is complete, an expansion for $\phi_n^{el}(\tau)$ exists such that

$$\begin{aligned}\phi_n^{el}(\tau) &= (1-P_{12})[\psi_+^{(1)}(\vec{r}_2-\vec{r}_b)\psi_{n*}(\vec{r}_1-\vec{r}_a) \\ &\quad + A(R)\psi_+^{(2)}(\vec{r}_2;\vec{R})\psi_{2s}(\vec{r}_1-\vec{r}_b)] \\ &= \sqrt{2[1+A(R)^2]}\sum_{n'} a_{n'}^{n}(R_o,R)\psi^{n'}(\vec{r}_1,\vec{r}_2;\vec{R_o}),\end{aligned} \tag{31}$$

where

$$a_{n'}^{n}(R_o,R) = \sqrt{\frac{1}{2[1+A(R)^2]}}(\langle \phi_n^{el};R|\psi^{n'};R_o\rangle).$$

To manipulate this expression further, we need to discuss the solutions $\psi^{n'}(\vec{r}_1,\vec{r}_2;\vec{R})$ of the Schrödinger equation for the Born-Oppenheimer Hamiltonian in more detail. The frozen nuclei equation has been studied extensively in the literature and very accurate eigenstates can be obtained. However, since our primary goal is not accuracy, for clarity we will take the eigenstates to be given by a linear combination of two atomic orbitals that are variationally optimized in the physically reasonable two-dimensional subspace to give the best approximation to the excited state in question. Therefore, we define molecular orbitals in the form [10]

$$\begin{aligned}\psi^{n'}(\vec{r}_1,\vec{r}_2;\vec{R_o}) &= \psi_{n'}(\vec{r_1};\vec{R_o})\psi_{21}(\vec{r_2};\vec{R_o}) \\ &\quad - \psi_{n'}(\vec{r_2};\vec{R_o})\psi_{21}(\vec{r_1};\vec{R_o}),\end{aligned} \tag{32}$$

where

$$\begin{aligned}\psi_{n'}(\vec{r};\vec{R_o}) &= [a_1^{n'}(R_o)\psi_{\mathrm{Li}}^{(n')}(\vec{r};R_o)+a_2^{n'}(R_o)\psi_{\mathrm{H}}^{(n')}(\vec{r};R_o)], \\ \psi_{21}(\vec{r};R_o) &= [b_1(R_o)\psi_{\mathrm{Li}}^{(2s)}(\vec{r};R_o)+b_2(R_o)\psi_{\mathrm{H}}^{(1s)}(\vec{r};R_o)].\end{aligned} \tag{33}$$

These molecular orbitals correspond to the electronic states that belong to the $\sigma(2s)ns\sigma$ electronic configuration. In Eqs. (32) and (25), exchange is *no longer* neglected and the electrons are placed into an antisymmetric spatial configuration that is demanded by a triplet state:

$$\psi^{n'}(\vec{r_1},\vec{r_2};\vec{R}_o) = -\psi^{n'}(\vec{r_2},\vec{r_1};\vec{R}_o). \tag{34}$$

The molecular orbitals in Eq. (33) for each fixed value of the principal quantum number, n', describe two different separated-atom limits. The more stable combination, $\mathrm{Li}(n'l)+\mathrm{H}(1s)$,[5] corresponds to a lithium atom in an excited state and a hydrogen atom in the ground state and is described by

$$\lim_{R\to\infty} a_1^{n'}(R)=1, \quad \lim_{R\to\infty} a_2^{n'}(R)=0,$$

$$\lim_{R\to\infty} b_1(R)=0, \quad \lim_{R\to\infty} b_2(R)=1. \tag{35}$$

The excited-state configuration, $\mathrm{Li}(2s)+\mathrm{H}(n')$, corresponds to a repulsive state and has the following limiting behavior:

$$\lim_{R\to\infty} a_1^{n'}(R)=0, \quad \lim_{R\to\infty} a_2^{n'}(R)=1,$$

$$\lim_{R\to\infty} b_1(R)=1, \quad \lim_{R\to\infty} b_2(R)=0. \tag{36}$$

Now, by means of the following device which exploits these separated-atom limits of the adiabatic wave functions, we can simplify Eq. (31) and ultimately derive an expression for the mixing coefficient $A(R)$. First, since the set of adiabatic states is complete for every internuclear separation, for any R' that differs from R_o an expansion exists such that

$$\phi_n^{el}(\tau) = \sqrt{2[1+A(R)^2]}\sum_{n'} a_{n'}^{n}(R',R)\psi^{n'}(\vec{r}_1,\vec{r}_2;\vec{R'}). \tag{37}$$

Accordingly, we can imagine writing equations identical to Eq. (37) for each internuclear separation inside an interval $(0,R_{max})$ and then summing them up. However, since R is a continuous parameter, this summation is actually an integration and we obtain

$$\begin{aligned}&\frac{R_{max}}{\sqrt{2[1+A(R)^2]}}(1-P_{12})[\psi_+^{(1)}(\vec{r}_2-\vec{r}_b) \\ &\quad \times \psi_{n*}(\vec{r}_1-\vec{r}_a)|_{0<|\vec{r}_1-\vec{r}_b|<\eta} \\ &\quad + A(R)\psi_+^{(2)}(\vec{r}_2;\vec{R})\psi_{2s}(\vec{r}_1-\vec{r}_b)|_{0<|\vec{r}_1-\vec{r}_b|<\eta}] \\ &\quad = \int_0^{R_{max}}\sum_{n'} a_{n'}^{n}(R,R')\psi^{n'}(\vec{r}_1,\vec{r}_2;\vec{R'})dR' \\ &\quad = \int_0^{R_{max}} a_n^{n}(R,R')\psi^{n}(\vec{r}_1,\vec{r}_2;\vec{R'})dR' \\ &\quad + \sum_{n'\neq n}\int_0^{R_{max}} a_{n'}^{n}(R,R')\psi^{n'}(\vec{r}_1,\vec{r}_2;\vec{R'})dR',\end{aligned} \tag{38}$$

where $\psi^{n}(\vec{r}_1,\vec{r}_2;\vec{R})$ is the adiabatic eigenstate that converges to the $\mathrm{Li}(ns)+\mathrm{H}(1s)$ configuration in the separated-atom

[5]The atomic lithium spectrum reveals that only the *s*-wave quantum defect differs significantly from zero. Therefore, all states with $l\neq 0$ can be considered quasidegenerate and they can be characterized simply with the principal quantum number n'.

limit.[6] Adjusting terms further and dividing through by R_{max} we get

$$\begin{aligned}\frac{1-P_{12}}{\sqrt{2[1+A(R)^2]}}&[\psi_+^{(1)}(\vec{r}_2-\vec{r}_b)\psi_{n*}(\vec{r}_1-\vec{r}_a)|_{0<|\vec{r}_1-\vec{r}_b|<\eta}\\&+A(R)\psi_+^{(2)}(\vec{r}_2;\vec{R})\psi_{2s}(\vec{r}_1-\vec{r}_b)|_{0<|\vec{r}_1-\vec{r}_b|<\eta}]\\&=\frac{1}{R_{max}}\int_0^{R_{max}}\psi^n(\vec{r}_1,\vec{r}_2;\vec{R'})dR'\\&+\frac{1}{R_{max}}\int_0^{R_{max}}[a_n^n(R,R')-1]\psi^n(\vec{r}_1,\vec{r}_2;\vec{R'})dR'\\&+\sum_{n'\neq n}\frac{1}{R_{max}}\int_0^{R_{max}}a_{n'}^n(R,R')\psi^{n'}(\vec{r}_1,\vec{r}_2;\vec{R'})dR'.\end{aligned}\tag{39}$$

The adiabatic electronic wave function for the Li(ns) + H($1s$) configuration in the separated-atom limit can be written as

$$\begin{aligned}\psi^n(\vec{r}_1,\vec{r}_2;R'\to\infty)=\frac{1}{\sqrt{2}}&[\psi_1^+(\vec{r}_2-\vec{r}_b)\psi_n(\vec{r}_1-\vec{r}_a)\\&-\psi_1^+(\vec{r}_1-\vec{r}_b)\psi_n(\vec{r}_2-\vec{r}_a)]\end{aligned}\tag{40}$$

and it can be verified that

$$\lim_{R'\to\infty}a_n^n(R,R')\simeq\frac{1}{\sqrt{1+A(R)^2}}\simeq 1.\tag{41}$$

This implies that the term $a_n^n(R,R')-1$ approaches zero as R gets larger and hence the second integral in Eq. (39) remains bounded. Furthermore, from the normalization condition

$$\sum_{n'}|a_{n'}^n(R,R')|^2=1,\tag{42}$$

we get, for $n'\neq n$,

$$\lim_{R'\to\infty}a_{n'}^n(R,R')=0,\tag{43}$$

thus the third integral in Eq. (39) also remains bounded. Therefore in the limit as R_{max} goes to infinity, the $1/R_{max}$ term forces the second and third expressions in Eq. (39) to be vanishingly small and we are left with a simple expression for the electronic wave function in the reaction zone in terms of the adiabatic states:

$$\begin{aligned}\frac{1-P_{12}}{\sqrt{2[1+A(R)^2]}}&[\psi_+^{(1)}(\vec{r}_2-\vec{r}_b)\psi_{n*}(\vec{r}_1-\vec{r}_a)|_{0<|\vec{r}_1-\vec{r}_b|<\eta}\\&+A(R)\psi_+^{(2)}(\vec{r}_2;\vec{R})\psi_{2s}(\vec{r}_1-\vec{r}_b)|_{0<|\vec{r}_1-\vec{r}_b|<\eta}]\\&=\lim_{R_{max}\to\infty}\frac{\int_0^{R_{max}}\psi^n(\vec{r}_1,\vec{r}_2;\vec{R'})dR'}{R_{max}}.\end{aligned}\tag{44}$$

Exploiting the orthonormalization condition on the core eigenstates, we can now obtain an expression for $A(R)$ in the form

$$\frac{A(R)}{\sqrt{2[1+A(R)^2]}}=\lim_{R_{max}\to\infty}\frac{\int_{|\vec{r}_1-\vec{r}_b|<\eta}\psi_{2s}(\vec{r}_1-\vec{r}_b)\int_{allspace}\psi_+^{(2)}(\vec{r}_2;\vec{R})^*\int_0^{R_{max}}\psi^n(\vec{r}_1,\vec{r}_2;\vec{R'})dR'd\vec{r}_2\vec{r}_1}{R_{max}\int_{|\vec{r}_1-\vec{r}_b|<\eta}|\psi_{2s}(\vec{r}_1-\vec{r}_b)|^2d\vec{r}_1}.\tag{45}$$

This is the main result of our derivations. Equation (45) shows that the essence of the information about the *entire* electronic structure of the molecule can be gained through integrations over a small region of space that picks out those special locations where the important many-body interactions occur. Our formalism provides a general recipe to locate these physically crucial poles, by means of a transformation between local and nonlocal representations for the electronic wave function, which also switches between a wave function that neglects exchange to one that accounts for exchange in the proper electronic symmetry. Note that the value of $A(R)$ reflects the properties of the nonlocal adiabatic wave function, $\psi^n(\vec{r}_1,\vec{r}_2;\vec{R'})$, in the finite region and this information is simultaneously being mapped from all internuclear separations through the integration over R', replacing a summation over a complete set of adiabatic states.

In the following section, we calculate the mixing coefficients for the excited triplet states of LiH. Then we use the mixing coefficient to determine an expression for the potential-energy curves for the motion of the nuclei. We also calculate the R-dependent quantum defects that were introduced in Eq. (22). Finally, we compare our results with accurate *ab inito* calculations and the Fermi approximation results.

[6] See Eq. (35).

TABLE I. Expansion coefficients for the effective molecular orbitals of LiH.

State	Effective molecular orbital
$3s^3\Sigma^+$	$0.0345\psi_{\mathrm{Li}}^{(n)}\psi_{\mathrm{Li}}^{(2s)}+0.6098\psi_{\mathrm{Li}}^{(n)}\psi_{\mathrm{H}}^{(1s)}+0.0094\psi_{\mathrm{H}}^{(n)}\psi_{\mathrm{Li}}^{(2s)}+0.0963\psi_{\mathrm{H}}^{(n)}\psi_{\mathrm{H}}^{(1s)}$
$4s^3\Sigma^+$	$0.0345\psi_{\mathrm{Li}}^{(n)}\psi_{\mathrm{Li}}^{(2s)}+0.5921\psi_{\mathrm{Li}}^{(n)}\psi_{\mathrm{H}}^{(1s)}+0.0094\psi_{\mathrm{H}}^{(n)}\psi_{\mathrm{Li}}^{(2s)}+0.1504\psi_{\mathrm{H}}^{(n)}\psi_{\mathrm{H}}^{(1s)}$
$5s^3\Sigma^+$	$0.0344\psi_{\mathrm{Li}}^{(n)}\psi_{\mathrm{Li}}^{(2s)}+0.5679\psi_{\mathrm{Li}}^{(n)}\psi_{\mathrm{H}}^{(1s)}+0.0112\psi_{\mathrm{H}}^{(n)}\psi_{\mathrm{Li}}^{(2s)}+0.2214\psi_{\mathrm{H}}^{(n)}\psi_{\mathrm{H}}^{(1s)}$
$7s^3\Sigma^+$	$0.0337\psi_{\mathrm{Li}}^{(n)}\psi_{\mathrm{Li}}^{(2s)}+0.5022\psi_{\mathrm{Li}}^{(n)}\psi_{\mathrm{H}}^{(1s)}+0.0157\psi_{\mathrm{H}}^{(n)}\psi_{\mathrm{Li}}^{(2s)}+0.3853\psi_{\mathrm{H}}^{(n)}\psi_{\mathrm{H}}^{(1s)}$
$9s^3\Sigma^+$	$0.0318\psi_{\mathrm{Li}}^{(n)}\psi_{\mathrm{Li}}^{(2s)}+0.5016\psi_{\mathrm{Li}}^{(n)}\psi_{\mathrm{H}}^{(1s)}+0.0219\psi_{\mathrm{H}}^{(n)}\psi_{\mathrm{Li}}^{(2s)}+0.3945\psi_{\mathrm{H}}^{(n)}\psi_{\mathrm{H}}^{(1s)}$
$12s^3\Sigma^+$	$0.0335\psi_{\mathrm{Li}}^{(n)}\psi_{\mathrm{Li}}^{(2s)}+0.4906\psi_{\mathrm{Li}}^{(n)}\psi_{\mathrm{H}}^{(1s)}+0.0185\psi_{\mathrm{H}}^{(n)}\psi_{\mathrm{Li}}^{(2s)}+0.4072\psi_{\mathrm{H}}^{(n)}\psi_{\mathrm{H}}^{(1s)}$

IV. RESULTS

We compute the potential-energy curves for the LiH $^3\Sigma^+$ $\sigma(2s)ns\sigma$ configuration from

$$U(R)=\frac{\langle\psi^{el}|\mathcal{H}|\psi^{el}\rangle}{\langle\psi^{el}|\psi^{el}\rangle}, \tag{46}$$

where ψ^{el} is given by Eq. (3). The numerical values for $A(R)$ are obtained from Eq. (45). We simplify our equations by noting that the atomic orbitals in Eq. (33) vary slowly with R', thus we treat them as constants in the integration over R' in Eq. (45), fixed at the internuclear separation, R, of the ion-core electronic wave functions:

$$\begin{aligned}\int_0^{R_{max}}&\psi^n(\vec{r}_1,\vec{r}_2;\vec{R'})dR'\\ &=\int_0^{R_{max}}[\psi_n(\vec{r}_1;\vec{R'})\psi_{21}(\vec{r}_2;\vec{R'})\\ &-\psi_n(\vec{r}_2;\vec{R'})\psi_{21}(\vec{r}_1;\vec{R'})]dR'\\ &\simeq\int_0^{R_{max}}(1-P_{12})\{[a_1^n(R')\psi_{\mathrm{Li}}^{(n)}(\vec{r}_1;R)\\ &+a_2^n(R')\psi_{\mathrm{H}}^{(n)}(\vec{r}_1;R)][b_1(R')\psi_{\mathrm{Li}}^{(2s)}(\vec{r}_2;R)\\ &+b_2(R')\psi_{\mathrm{H}}^{(1s)}(\vec{r}_2;R)]\}dR'.\end{aligned} \tag{47}$$

Then, for R_{max} chosen sufficiently large, the limit-integral expression of Eq. (44) becomes an average over the variational coefficients of the adiabatic wave functions. After the integration is executed we obtain an effective molecular orbital which must be matched to the two-channel electronic wave function in the excitation region:

$$\begin{aligned}\psi_{ad}(\tau)=(1-P_{12})(&a\psi_{\mathrm{Li}}^{(n)}\psi_{\mathrm{Li}}^{(2s)}+b\psi_{\mathrm{Li}}^{(n)}\psi_{\mathrm{H}}^{(1s)}\\ &+c\psi_{\mathrm{H}}^{(n)}\psi_{\mathrm{Li}}^{(2s)}+d\psi_{\mathrm{H}}^{(n)}\psi_{\mathrm{H}}^{(1s)}).\end{aligned} \tag{48}$$

The expansion coefficients in this expression for different electronic states of LiH are listed in Table I. In our calculations we set $R_{max}=70$ bohr, but this value should be increased if greater accuracy is desired. The ion-core potential-energy curve, $E_1^+(R)$, has been calculated, consistent with the assumptions of our theory, by placing the valence electron in the ground-state atomic orbital of hydrogen,

$$\psi_1^+(\vec{r}_2-\vec{r}_b)=\psi_{\mathrm{H}}^{1s}(\vec{r}_2-\vec{r}_b), \tag{49}$$

and employing

$$E_1^+(R)=\langle\psi_{\mathrm{H}}^{1s}(\vec{r_2}-\vec{r}_a)|\mathcal{H}_2|\psi_{\mathrm{H}}^{1s}(\vec{r_2}-\vec{r}_a)\rangle. \tag{50}$$

Similarly, the excited-state ion-core potential-energy curve was generated by constructing a Schmidt orthonormalized electronic wave function with dominant lithium ground-state character,

$$\psi_2^+(\vec{r_2};\vec{R})=\frac{1}{\sqrt{1-S(R)^2}}[\psi_{\mathrm{Li}}^{2s}(\vec{r}_2-\vec{r}_a)-S(R)\psi_{\mathrm{H}}^{1s}(\vec{r}_2-\vec{r}_b)],$$

$$S(R)=\langle\psi_{\mathrm{H}}^{1s}|\psi_{\mathrm{Li}}^{2s}\rangle, \tag{51}$$

and using Eq. (50) with ψ_1^+ replaced by ψ_2^+. The ion-core potential-energy curves, $E_1^+(R)+1/R$ and $E_2^+(R)+1/R$, calculated in this fashion, have been plotted in Figs. 3(a) and 3(b).

A. Calculation of the integration range η

In Eq. (45) the term $\int_{|\vec{r}_1-\vec{r}_b|<\eta}|\psi_{2s}(\vec{r}_1-\vec{r}_b)|^2d\vec{r}_1$ acts as a normalization constant in the reaction zone. The sphere of radius η is the region of space where the hydrogenic excitation takes place and thus one expects significant overlap between the ground-state hydrogen wave function and the first excited state in this volume. A measure of this overlap is given by

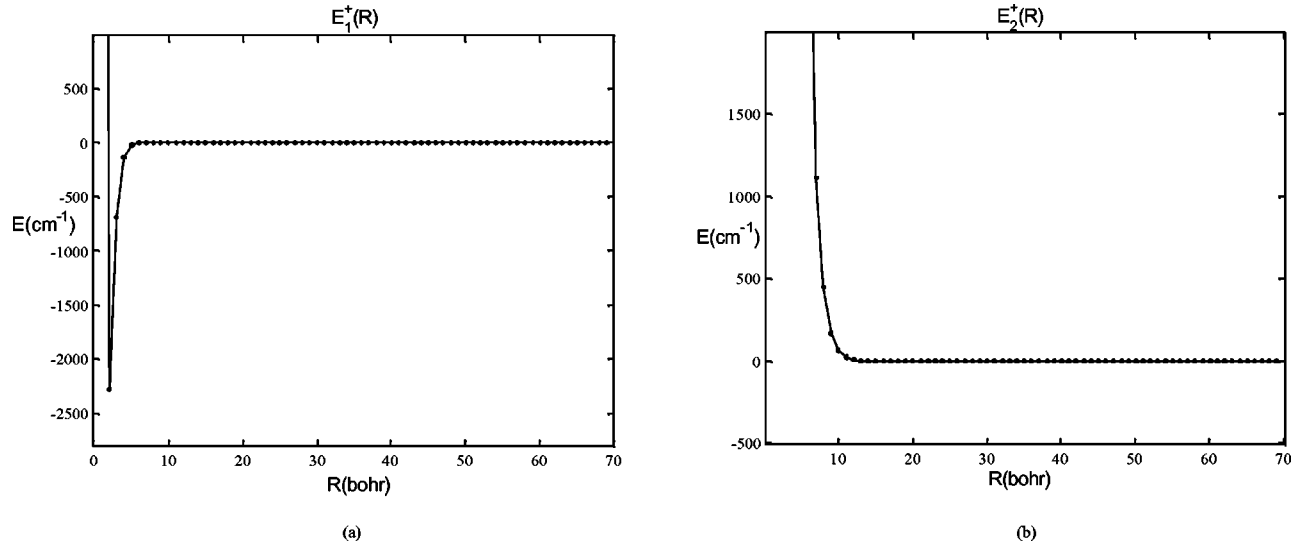

FIG. 3. The ion-core potential-energy curves $E_1^+(R)+1/R$ and $E_2^+(R)+1/R$.

$$\int_{|\vec{r}_1-\vec{r}_b|<\eta} \psi_{2s}^{\mathrm{H}}(\vec{r}_1-\vec{r}_b)\,\psi_{1s}^{\mathrm{H}}(\vec{r}_1-\vec{r}_b)\,d\vec{r}_1 \tag{52}$$

and the approximate region in which this overlap is significant can be calculated by letting

$$f(k)=\int_{|\vec{r}_1-\vec{r}_b|<k} |\psi_{2s}^{H}(\vec{r}_1-\vec{r}_b)|^2 d\vec{r}_1,$$

$$g(k)=\int_{|\vec{r}_1-\vec{r}_b|<k} \psi_{2s}^{\mathrm{H}}(\vec{r}_1-\vec{r}_b)\,\psi_{1s}^{\mathrm{H}}(\vec{r}_1-\vec{r}_b)\,d\vec{r}_1, \tag{53}$$

and solving for η from

$$f(k)=g(k). \tag{54}$$

The value of η from Eq. (54) comes out to be 3.46 bohr. Physically, Eq. (54) ensures that η provides a numerical scale for the region where the excitation occurs. The excitation process takes place in the innermost region occupied by the hydrogen atom ground state. The probability amplitude for the excitation will be proportional to the off-diagonal matrix element of $1/r_{12}$ and this matrix element accumulates in the reaction zone and dominates all other interactions. At $r_{1b}>\eta$, the total electronic probability in the excited state, $f(k)$, exceeds the overlap of the excited state with the ground state, therefore in this region to a good approximation many interactions can be turned off and the electronic wave function can be taken in the representation of Eq. (3).

The method for choosing η presented here is not unique and other schemes for determining η can be proposed. It is possible to let η be energy dependent and vary state to state. This may lead to more accurate results. However, the method presented here is mathematically explicit and physically sensible. Furthermore, fixing η for all states allows for a calculation of the global electronic structure and obviates the need for state by state analysis.

1. $3s\,^3\Sigma^+$ *state*

In Fig. 4(a), we have plotted the calculated potential-energy curve given by Eq. (46). Comparison with *ab initio* results [11] shows good qualitative agreement between the two approaches. Our plot displays a barrier with maximum at 7.5 bohr and height 192 cm^{-1}. The barrier is followed by a well with minimum approximately at 3.8 bohr and depth 2050 cm^{-1}. The barrier maximum from the *ab initio* results is at $R=9.05$ bohr and the height is at 249 cm^{-1}. However, the additional shallow well that arises at larger R than the barrier in Fig. 4(a) is absent in the *ab initio* results. The height of the barrier is underestimated in our model because of the neglect of the additional repulsive interactions that arise in the Li^+ core and the reaction zone, namely, the off-diagonal matrix elements of $1/r_{12}$ which are scaled by $A(R)$. We expect these interactions to be significant for this low-lying state. The maximum of the outer barrier in Ref. [1] appears at $R\sim 8$ bohr closer to the value reported in Ref. [11], with a difference of 1 bohr. However, the height of the barrier is overestimated in this model by a factor of 1.2. This difference can be explained from the use of the zero energy scattering length in the Fermi approximation [1].

The R-dependent quantum-defect curve for the Lithium atom, defined by Eq. (22), is shown in Fig. 5(a). It is seen that the quantum defect starts at 0.397 near $R=6$,[7] and then converges toward the atomic value of $\mu=0.4$ as the internuclear separation increases. The analogous plot for the hydrogenic excitation process in Fig. 5(b) recovers a quantum defect that remains constant at -0.15 beyond $R=8$. Here, the change from the ground-state quantum number $n=1$ toward the noninteger value of 1.15 can be interpreted as a signature of the excitation of the hydrogen atom. In Fig. 4(c), we plot the mixing coefficient $A(R)$, the shape of which displays a correspondence with the $3s$ potential-energy curve. This resemblance underlines the fact that all the finer features of the

[7]Recall that our calculations are valid for $R>4$ bohr.

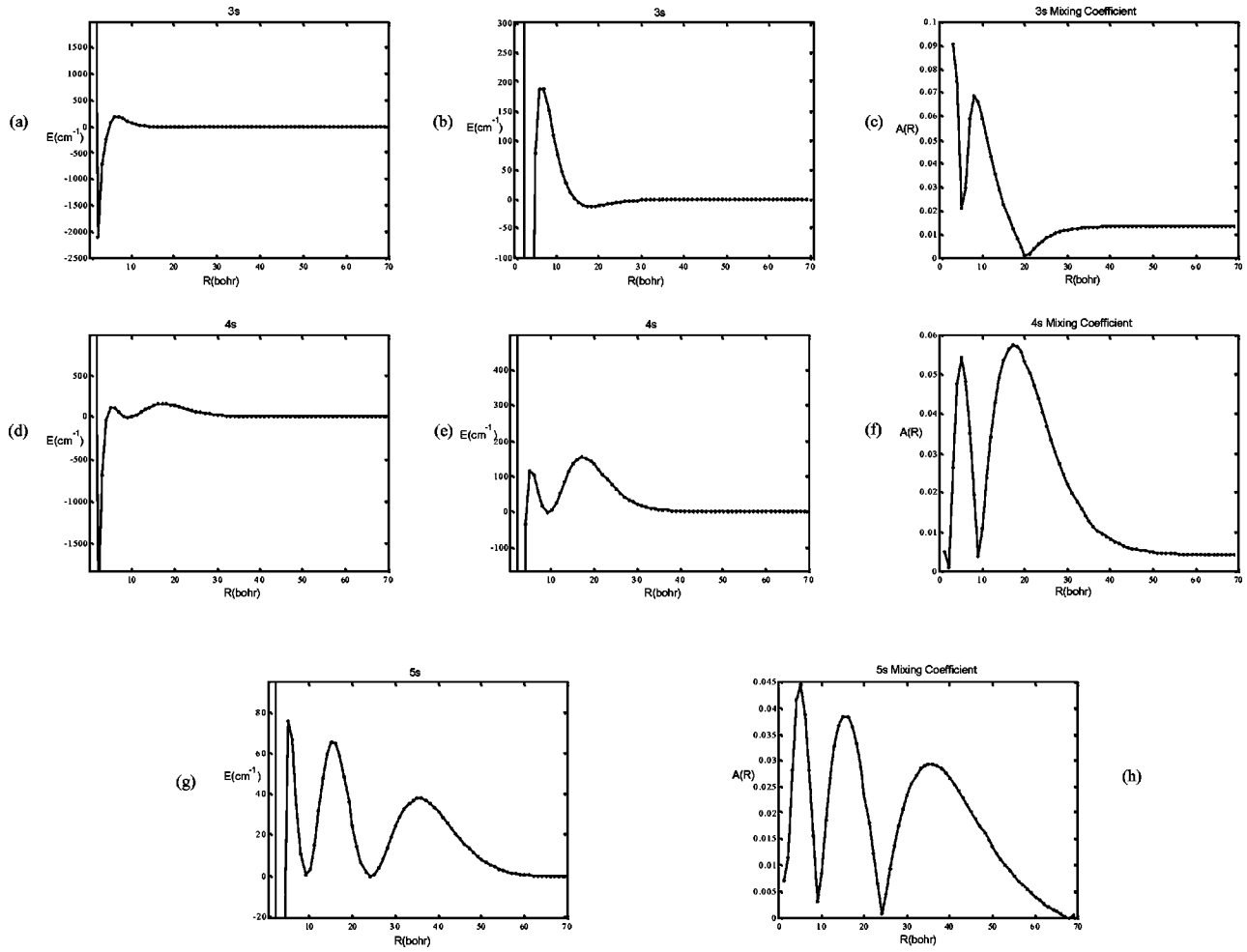

FIG. 4. Potential-energy curves of LiH. The potential-energy curves plotted in the figure correspond to the $3s\,^3\Sigma^+$, $4s\,^3\Sigma^+$, and $5s\,^3\Sigma^+$ states, respectively. Comparison with the curves in Ref. [9] shows an overall qualitative agreement with *ab inito* calculations. The mixing coefficients for each state are also plotted in the third column, and they display a clear resemblance in shape to the corresponding potential-energy curves. This shows that the physical origins of the finer features of the potential-energy curves are reflected by the numerical values of the mixing coefficients in our theory.

potential-energy curves are obtained from the mixing coefficient.

2. $4s\,^3\Sigma^+$ *state*

Figure 4(d) shows that the overall features of the *ab initio* results of Ref. [11] have been captured closely for this state within our treatment. There is a secondary minimum at about $R_{min}=10$ bohr, which is followed by a barrier with maximum appearing at $R_{max}=18$ bohr as compared to the *ab initio* values of $R_{min}=11$ bohr and $R_{max}=18$ bohr. Our calculation overestimates the height of the inner and outer barriers at 105 cm^{-1} and 160 cm^{-1}. The reported values from Ref. [11] are, respectively, 60 cm^{-1} and 62 cm^{-1}. The Fermi approximation also overestimates the height of the innermost maximum at nearly 115 cm^{-1}. The error in our calculation is most likely due to the use of the limited basis set in Eq. (33) and to the neglect of the additional channels that describe electron-hydrogen scattering in Eq. (25). Further comparison to the Fermi approximation result shows that some of the finer details of the potential energy curve have been captured in our results, such as the ratio of the heights of the inner and outer maxima. This may be due to the additional flexibility of our formalism, namely, the treatment of the hydrogen atom as a dynamical object instead of a frozen, passive perturber. As shown in Fig. 5(c), the quantum-defect curve that describes the Li^+-electron interaction has more oscillations and the oscillations have larger amplitude than the $3s$ curve about its atomic value of $\mu=0.4$. At $R=18$ bohr, it falls as low as 0.367. These oscillations are related to the undulations observed in the PECs at long range and they indicate a stronger coupling between the two electronic channels. This is further verified from the quantum-defect curve for hydrogenic excitation in Fig. 5(d), which converges to a more negative value of -0.209 (rather than -0.15 as for $3s$) beyond $R=10$ bohr. The larger absolute magnitude of the quantum defect in the hydrogen channel for the $4s$ state than its value for the $3s$ state shows that hydrogenic excitation is becoming more significant for higher electronic states.

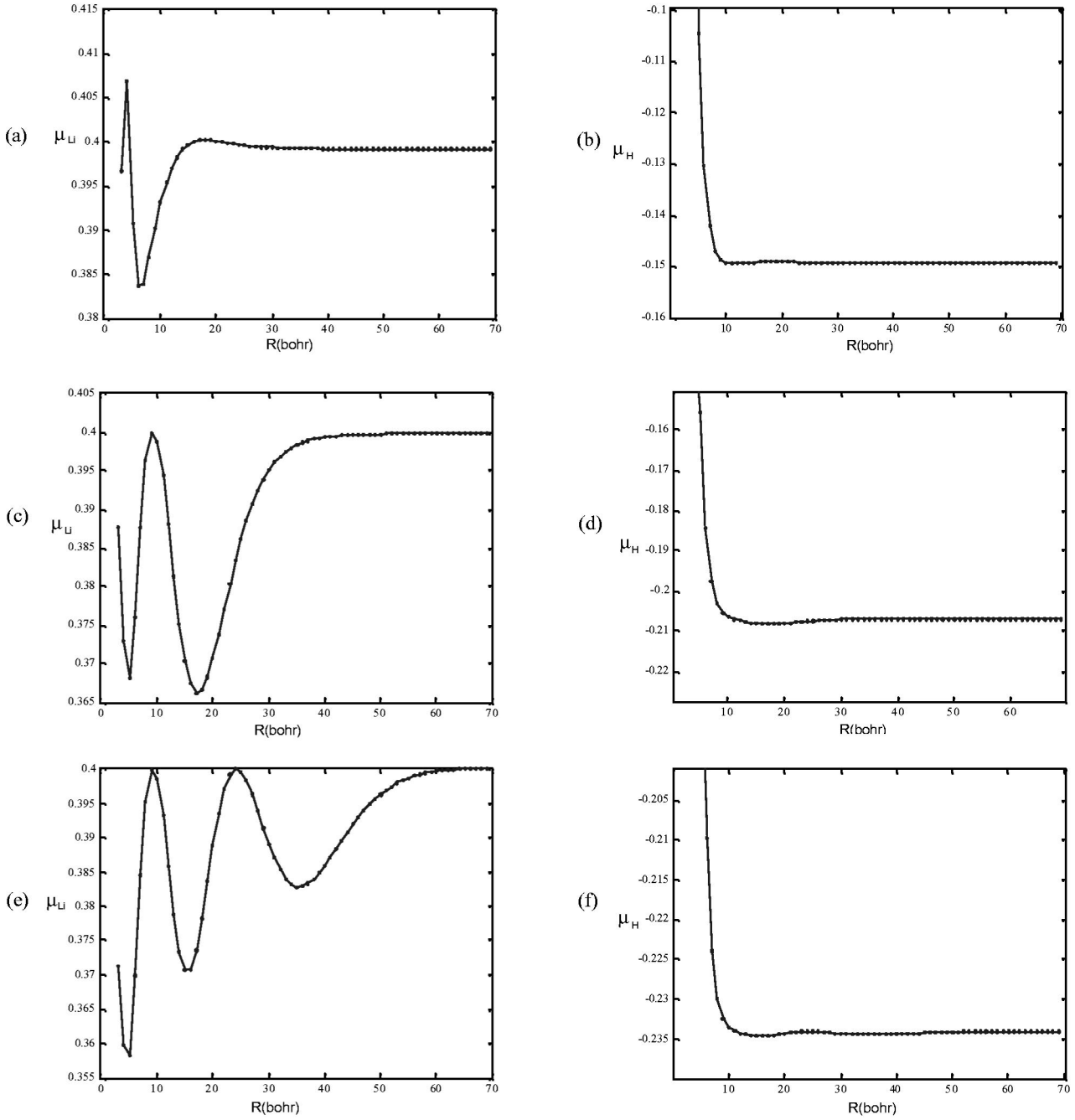

FIG. 5. The quantum-defect curves for the lithium and the hydrogen channels.

3. $5s\,^3\Sigma^+$ *state*

The calculated potential-energy curve for this state is plotted in Fig. 4(g). The correct number of wells and barriers is reproduced, the locations of the corresponding minima and maxima are in good agreement with the *ab initio* results. The only significant discrepancy seems to be in the barrier heights. The height of the first barrier at 79 cm^{-1} is smaller than the *ab initio* value of 100 cm^{-1}. The heights of the second and third barriers are 68.3 cm^{-1} and 41 cm^{-1}. These exceed the *ab initio* barrier heights, which are 33 cm^{-1} and 21 cm^{-1}, respectively. The discrepancies may be related to the use of a limited basis set in Eq. (33) and the neglect of the channels describing hydrogen-electron scattering in Eq. (25).

4. Higher electronic states and the Rydberg scaling law

In Fig. 6, we have plotted the potential-energy curves for the $n=7$, $n=9$, and $n=12$ electronic states that were calculated using the bound space integration formula. In these potential-energy curves, oscillations and undulations are seen even at very large internuclear separation. This is due to the increasing diffuseness and the increasing number of radial nodes of the atomic orbitals on the lithium atom at higher

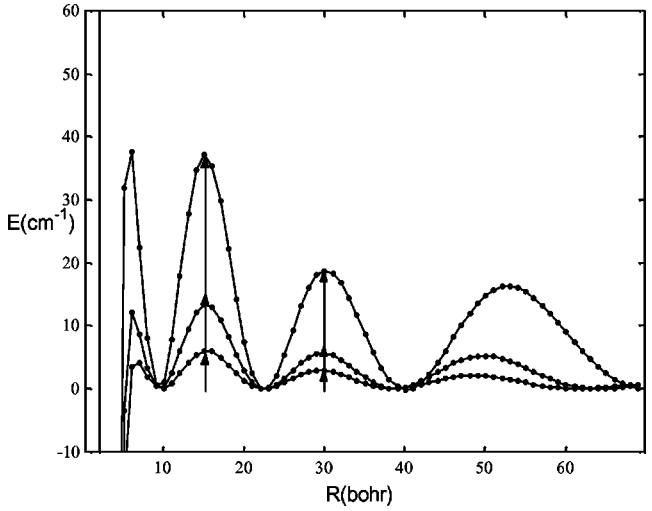

FIG. 6. Higher electronic states and $(n^*)^{-3}$ scaling law. For these high electronic states, oscillations and undulations in potential curves are seen even at very large internuclear separation. The amplitudes inside each of the barriers in the potential-energy curves are proportional to the inverse cube of the principal quantum number and the corresponding barriers line up. This suggests that for these highly excited states, the shapes of the potential-energy curves are essentially governed by the simple Rydberg scaling laws.

excitation. Furthermore, the amplitudes a inside each of the barriers in the potential-energy curves, indicated by the upward pointing arrows in Fig. 6, follow very closely a simple scaling law:

$$a \propto \left(\frac{1}{n^*}\right)^3,$$

$$n^* = n - 0.4, \tag{55}$$

where n^* is the effective principal quantum number for the lithium atom. This scaling law is related to the diagonal matrix elements of the $1/r_{12}$ operator in the basis of the Rydberg orbitals that are proportional to $(n^*)^{-3/2}$ and is known as the Rydberg scaling law. Figure 6 shows that for highly excited electronic states, the shapes of the potential-energy curves (including the nontextbook oscillations) are essentially governed by the simple Rydberg scaling laws.

Table I provides further physical insight into the triplet states of LiH. Although the electronic structure is dominated by the $\mathrm{Li}^{ns}\mathrm{H}$ term in the effective molecular orbital, an additional term occurs in the form of $d\psi_{\mathrm{H}}^{(n)}\psi_{\mathrm{H}}^{(1s)}$ that describes $\mathrm{Li}^+\mathrm{H}+e$ character in the electronic wave function. The existence of this term implies that the triplet state is reached by the formation of an intermediate $\mathrm{H}+e$ type species in the triplet symmetry, as the electron, initially localized on the lithium atom, scatters off the hydrogen atom.

V. DETAILS AND THE LIMITATIONS OF THE CALCULATION

The minimum value of internuclear distance R. The minimum value of R is chosen such that the overlap integral $S(R)$ of a $2s$-type lithium atomic orbital and a $1s$ hydrogenic orbital is sufficiently small for the desired accuracy. For $R>4$, $|S(R)|<0.01$ and rapidly approaches zero for increased values of R. For R less than this threshold, electron correlation effects become significant and the off-diagonal matrix element of the electron-electron Coulomb repulsion term in Eq. (7) cannot be approximated to zero. A more sophisticated calculation is needed for a description of the two-electron wave function when R is smaller than this threshold value.

Li^+*-electron interaction.* Equation (2) describes the interaction of the Rydberg electron with Li^+ in the central field approximation with optimized parameters that give the closest agreement with the observed quantum defects in the ns Rydberg series of Li. Altering these parameters changes the nodal structure of the diffuse Rydberg orbitals on Li and this leads to significant changes in the resultant potential-energy curves. Other forms for the interaction of the electron with Li^+ can be used, but it is important that any adjustable parameters are optimized *a priori*.

Restriction to triplet states. Our calculations are restricted to a study of the triplet states because the approximate electronic wave function in Eq. (3) is expected to realistically describe the adiabatic curves in the triplet electronic symmetry. For singlet states, additional complications occur due to the interactions with the ionic state dissociating to $\mathrm{Li}^+ + \mathrm{H}^-$. These interactions lead to multiple avoided crossings in the potential-energy curves and more flexibility is required in Eq. (3) to capture this behavior. One feasible extension in this direction is to allow for the mixing in of a third state, at each internuclear distance R, that will correspond to a $\mathrm{Li}^+\mathrm{H}^-$ formation. This procedure requires further study and constitutes a natural next step in the development of our method.

VI. CONCLUSIONS

In this work, we have demonstrated that the essential qualitative features of the potential-energy curves for the low-lying $ns\,^3\Sigma^+$ electronic states of LiH can be reproduced and that the potential curves for higher-Rydberg states can be obtained in a unified way with our finite-space bounded integration method. The main idea behind our theory is the delineation of the dominant physical processes that occur within a bounded region of space. The information about these physical processes is then captured into an electronic wave function, which is a solution of the Schrödinger equation in the outer region using the bound space integration formula of Eq. (45).

For the case of LiH, the analysis reveals that neither of the nuclei acts completely as a static perturber for the other one, and electronic energy gets transferred between them by means of the excitation of the hydrogen atom to its first excited state. The physical interaction that is responsible for the excitation is the electron-electron repulsion $1/r_{12}$ term in the Hamiltonian. When the two electrons are within the effective interaction length for atomic hydrogen, this term dominates all other electrostatic interactions that could contribute to the excitation of the hydrogen atom. Since the hydrogen atom is initially in its ground state, this process must

occur inside a small sphere centered on the hydrogen with radius given by the excitation radius η. Exchange becomes significant when the two electrons are close to each other, and hence the solutions that are valid inside the finite region of space must be antisymmetrized. In this manner, the information about the triplet nature of the electronic wave function is mapped into the exchange-neglected representation in Eq. (3) by means of Eq. (45).

The developed technique also provides a recipe to inject information from the exact representations of many-body electronic wave functions into simplified representations through integrations in finite regions of space where the electron pair interaction is important. Significant improvement in the accuracy of our results may be achieved, if our picture is built upon exact *ab initio* results instead of the approximate adiabatic wave functions used here.

The current theory can be expected to produce similarly accurate results for other hydrides with more complicated hydrogen partners, to the extent that the atomic ion core of the hydrogen partner can be treated as ''frozen'' and its interaction with the Rydberg electron can be well approximated with a central field. The extension of the method to nonhydrides seems quite feasible provided the perturbing atom has energetically accessible excited states. For example, we expect the method to generalize in a straightforward fashion to LiHe or Li_2.

Our method can also be employed to obtain the potential curves for the states belonging to different Rydberg series of LiH. Subsequently, these potential curves can be drawn on for the determination of the quantum-defect curves and their energy dependence [3]. Following the work of Ross and Jungen, we plan to progress toward such a generalization with the ultimate goal of obtaining the set of quantum-defect functions that will provide a complete description of the short-range scattering processes.

ACKNOWLEDGMENTS

This research was supported by NSF Grant No. CHE-0104197. We thank Professor Jianshu Cao and Professor Christian Jungen for helpful discussions, particularly the suggestion that any approximate theory for Rydberg electronic structure and dynamics should be valid for all n and become increasingly accurate at high n^*.

[1] A.S. Dickinson and F.X Gadèa, Phys. Rev. A **65**, 052506 (2002).
[2] M. Arif, Ch. Jungen, and A.L. Roche, J. Chem. Phys. **106**, 4102 (1997).
[3] S.C. Ross and Ch. Jungen, Phys. Rev. A **49**, 4353 (1994).
[4] U. Fano, Phys. Rev. A **2**, 353 (1970).
[5] M.J. Seaton, Rep. Prog. Phys. **46**, 167 (1983).
[6] Michael Courtney, Neal Spellmeyer, Hong Jiao, and Daniel Kleppner, Phys. Rev. A **51**, 3604 (1995).
[7] Johannes Stiehler and Jurgen Hinze, J. Phys. B **28**, 4055 (1995).
[8] O. Atabek and Ch. Jungen, J. Chem. Phys. **66**, 5584 (1977).
[9] C. Schwartz, Phys. Rev. **124**, 1468 (1961).
[10] Donald A. McQuarrie, *Quantum Chemistry* (University Science Books, California, 1983).
[11] Alexandra Yiannopoulou, Gwang-Hi Jeung, Su Jin Park, Hyo-Sug Lee, and Yoon Sup Lee, Phys. Rev. A **59**, 1178 (1999).
[12] C. Bordas, P. Labastie, J. Chevaleyre, and M. Broyer, J. Chem. Phys. **129**, 21 (1989).